Available online at www.sciencedirect.com

ScienceDirect

PHOTONICS AND NANOSTRUCTURES Fundamentals and Applications

Photonics and Nanostructures – Fundamentals and Applications 12 (2014) 493–500

www.elsevier.com/locate/photonics

Comparison of nano-structured solar cell anti-reflection coating based on graded-index or mode coupling approach

Albert Lin *, Yan-Kai Zhong, Sze-Ming Fu

Department of Electronic Engineering, National Chiao-Tung University, Hsinchu 30010, Taiwan

Received 7 September 2013; received in revised form 12 July 2014; accepted 5 August 2014
Available online 19 August 2014

Abstract

Solar cell nano-structured anti-reflection coatings based on graded index (GI) and mode coupling are all proposed to significantly reduce the reflection from semiconductor–air interface. In this work, it is shown that purely graded index approach can lead to degradation of long wavelength absorption by eliminating quasi-guided mode excitation. The reason is that the physically graded layer not only provides low reflectance path from air to semiconductor, but also from semiconductor to air, leading to photon escape. This results in out-coupling of photons from the semiconductor to air. On the other hand, anti-reflection coating based on mode coupling does not suffer from degraded long wavelength absorption and it is capable of acting as one-way photon pass coating. It is found that the sidewall thickness of mode coupling anti-reflection coating has significant impact on its effectiveness for anti-reflection, and therefore the selection of process methods is critical for its low reflectance. It is proposed that the purely graded index coating is more suitable for wafer-based photovoltaics where full absorption is possible by two photon traces. The mode coupling coating is suitable for both wafer-based photovoltaics and thin-film photovoltaics since it provides not only low reflectance but also long wavelength quasi-guided mode excitations. In the end, new types of anti-reflection coating and light trapping structure are proposed to further enhance the performance.

Keywords: Anti-reflection coating; Solar cell; Graded index; Mode coupling

1. Introduction

Photonic nano-structures have been emerging as promising candidates for anti-reflection (ARC) coatings. Specifically for solar cells, broadband low reflectance is the basic requirement for effective ARC to accommodate the broad solar spectrum. Several schemes are proposed, among which the most effective one shows decent broadband characteristics is so-called graded index (GI) approach. Anti-reflection coatings falling into this category includes dielectric multi-layer structures [1], semiconductor nano-tips [2], and closely related dielectric nano-structures [3,4] which can actually be regarded as a pseudo-graded index approach. In this work, it is going to show that while purely graded-index approach can provide broad-band low-reflectance characteristic, it can significantly degrade long wavelength waveguiding. This is because the low reflectance is based on physically graded index and, therefore, the low reflectance nature exists for both air to semiconductor and semiconductor to air incidence. Since photons can easily go through the graded index layer from semiconductor to air, they can

* Corresponding author. Tel.: +886 35712121.
E-mail address: hdtd5746@gmail.com (A. Lin).

http://dx.doi.org/10.1016/j.photonics.2014.08.002
1569-4410/

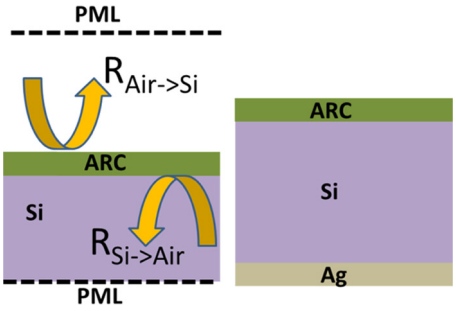

Fig. 1. The simulation structure for (left) the anti-reflection coating reflectance and (right) the solar cell absorbance.

easily escape the device leading to degraded long wavelength light trapping. Another category of anti-reflection coating does not count on physically graded material layers and instead it utilizes the mode coupling through the periodic grating structures on the solar cell front surface. This category includes ZnO nanorods [5], surface plasmon ARCs [6–9], grating couplers [10], and the recently proposed, very promising dielectric ARC based on Mie scattering [11]. It is shown here that ARC based on mode coupling is more robust to long wavelength absorbance degradation because the mode coupling ARC does not provide low reflectance path for photons coming from semiconductor to air. Therefore, it provides one-way photon pass, compared to the significant photon out-coupling resulted from the graded index ARC.

2. Geometry and simulation details

In this study the reflectance and absorbance are calculated for silicon solar cells with various nano-structured ARCs. The structure for absorbance calculation is ARC + 0.3 μmSi + Ag, while the structure for reflectance calculation is ARC + Si + perfectly matched layer (PML). It is a common practice to include only the front surface texture when comparing the effectiveness of anti-reflection characteristics [1–3,11].

The study of photon in- and out-coupling is done by calculating the reflectance from air through ARC to Si, and the reversed reflectance from Si through ARC to air, as illustrated in Fig. 1. When calculating the reversed reflectance, the imaginary part of silicon dielectric constant is neglected due to the constraint that the source region cannot be lossy. This practice has been employed in the literature [12]. In fact, the purpose of this work is studying the degradation of long wavelength guided modes, and the imaginary parts of dielectric constant at long wavelength are generally not very significant due to weak material absorption. It is going to show later that one-way photon pass is the key for anti-reflection coatings to have both low reflectance from air to semiconductor and strong quasi-guided modes at long wavelength to maintain solar cell light trapping.

In most of the solar cell technologies including wafer-based photovoltaics and multi-junction solar cells, the metal contact will be deposited through the vias in the insulating ARCs. In the case where transparent conducting contacts are needed, the ARCs materials presented in this paper can be replaced by transparent conducting oxide (TCO) such as indium tin oxide (ITO), aluminum doped zinc oxide (AZO), fluorine-doped tin oxide (FTO). Nevertheless, it should be pointed out that the comparison presented in this work, i.e., difference between graded index ARCs and mode coupling ARCs, will not change.

In this work, the choice of materials, i.e., SiO_2 TiO_2 Si_3N_4, is to align with the literature [1–3,11]. For wafer-based or multi-junction photovoltaics, insulators are frequently used as ARCs and the reflectance is more important since photons can be absorbed in one or two photon passes. For thin-film photovoltaics, TCOs are frequently used as ARCs and the absorbance is more important since the photons cannot be absorbed fully within two photon passes. In order to have a unified material selection and fair comparison, same ARC materials are used for both absorbance and reflectance calculations. Nevertheless, changing ARCs to other materials instead of what is used in this work will not change the key observation and conclusion presented here.

The absorbance is calculated by integrating the power dissipation in silicon:

$$A(\lambda) = \frac{1/2 \int_V \omega \varepsilon_0 \varepsilon''(\lambda) |\vec{E}(\vec{r})|^2 dv}{1/2 \int_S Re\{\vec{E}(\vec{r}) \times \vec{H}^*(\vec{r})\} \cdot d\vec{s}} \quad (1)$$

where ω is the angular frequency, λ is the free space wavelength, ε_0 is the permittivity in vacuum, and ε'' is the imaginary part of complex semiconductor dielectric constant. The normalized integrated absorbance can be defined to compare different ARCs. This is needed since the active silicon material volume might be different for various ARCs.

$$A_{Int} = \frac{V_{Si,Ref}}{V_{Si}} \frac{\int \frac{\lambda}{hc} \Omega(\lambda) A(\lambda) d\lambda}{\int \frac{\lambda}{hc} \Omega(\lambda) d\lambda} \quad (2)$$

where $V_{Si,Ref}$ is the silicon volume of one period (P) for the planar cell. In this study the silicon thickness is taken to be 0.3 μm and thus $V_{Si,Ref} = P \times P \times 0.3$ μm. V_{Si} is the silicon volume of one period for the solar cell structure with a specific front surface coating. $\Omega(\lambda)$ is the AM 1.5 solar spectrum in unit of $J\,s^{-1}\,cm^{-2}\,nm^{-1}$,

Fig. 2. Illustration of purely graded index ARC using planar multi-layer.

h is the Plank constant, λ is the free space wavelength, and c is the speed of light. The details for calculating absorbance can be found in Refs. [13–15]. The material optical constants are from Rsoft material database [16]. The calculation is conducted by Rsoft Diffractmod [16], which solves Maxwell's equations using a series expansion by waveguide modes.

3. Graded index approach

The geometry of the multi-layer dielectric ARC is from Ref. [1] where $t_1 = 200$ nm, $t_2 = 120$ nm, $t_3 = 45$ nm. When calculating the reflectance, the structure is ARC + Si + PML. The planar multi-layer is the most common ARC and layer-by-layer deposition can be employed to construct this type of structure. When calculating the absorbance, the structure is ARC + 0.3 μmSi + Ag reflector. Planar multi-layer dielectrics are the simplest form of graded index ARC as illustrated in Fig. 2. From Fig. 3, the reflectance is smaller than 5% except for the short wavelength. The improvement over a single layer dielectric ARC [1] is due to the interference effect initiated by the multiple dielectric interfaces and the compromise over the full spectral range. The reflectance can be further decreased by increasing the number of layers. For absorbance in Fig. 3, the mode excitation is very weak due to the easy-in-easy-out nature of planar multi-layer dielectrics, leading to photon escape. It should be pointed out that even without large angle diffraction, planar structure can exhibit strong-guided mode peaks by Fabry–Perot resonance [10,17]. Therefore, the graded-index ARC essentially eliminates the possibility of confined modes here due to significant photo out-coupling. This can be best reflected by computing the reflectance for the cases where photons are incident from air to Si and from Si to air, as illustrated in Fig. 3. The similar reflectance from Si to air and from air to silicon is due to the planar geometry. While the reflectance from air into silicon is lowered by ARC, the reflectance from silicon to air is also decreased significantly. This leads to the difficulty to trap the photons inside the silicon film, resulting in low absorbance for long wavelength as seen in Fig. 3. The normalized integrated absorbance is 0.119. The integrated metal loss is 0.061.

The geometry of silicon nano-tip ARC is from Ref. [2] where $L = 1.6$ μm and $P = 0.2$ μm. The ultra-long silicon nano-tips are formed by firstly depositing a self-assembled monolayer (SAM) of metal nano-particles. The metal nano-particle array then serves as an etching mask during anisotropic dry etching process. Finally, the metal particles are removed after silicon nano-tips are formed [2]. When calculating the reflectance, the structure is ARC + Si + PML. When calculating the absorbance, the structure is ARC + 0.3 μmSi + Ag reflector. Silicon or semiconductor nano-tip is the most famous example of graded index (GI) ARCs as illustrated in Fig. 4. The physically graded geometry leads to the grading of the effective index. Nonetheless, this effect is also dual-way since the photons incident from silicon to air also see the effective index grading. In Fig. 5, the reflectance of silicon nano-tip GI ARC is extremely low, <1% for the entire spectral range, reflecting the

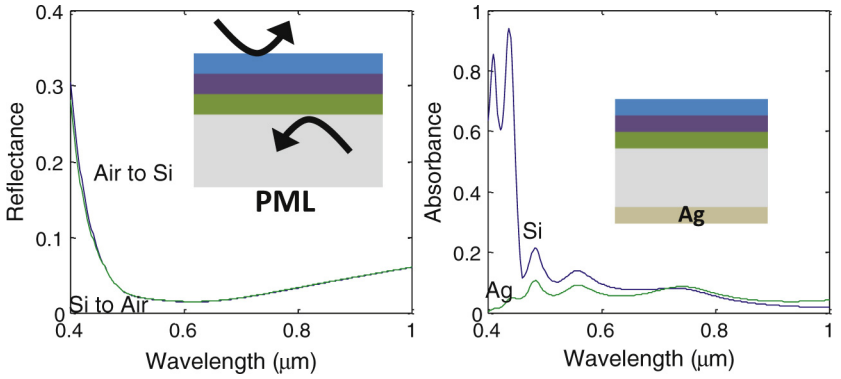

Fig. 3. Planar multi-layer purely GI ARC characteristic. (Left) reflectance from air to Si and reflectance from Si to air. (Right) absorbance for a stack of ARC, 0.3 μm Si and a silver reflector.

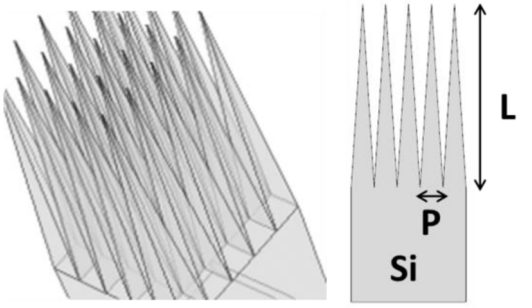

Fig. 4. Illustration of purely graded index ARC using silicon nanotips.

effectiveness of index grading. Nevertheless, the long wavelength quasi-guided mode excitations are annihilated, similar to the case of the planar multi-layer GI ARC where long wavelength absorption peaks are very weak. The photon escape also exists for silicon nano-tip ARC, due to its index grading using physically tapered geometry. The photon escape is particularly severe for long wavelength part of the spectrum, as illustrated the reflectance plot in Fig. 5. The normalized integrated absorbance is 0.160. The integrated metal loss is 0.051.

The dielectric nanotip ARC can be regarded as a pseudo graded index (GI) ARC because there exists a heterogeneous interface between dielectric/Si [3]. The perfect index grading from air to Si is broken at the dielectric/Si heterogeneous interface. The geometry of the dielectric nano-tip pseudo-GI ARC is $P = 600$ nm as illustrated in Fig. 6 [3]. Here the dielectric is chosen to be titanium oxide (TiO_2). The dielectric nano-tip ARC is not a purely GI approach since the index grading is discontinued at TiO_2–Si interface. The TiO_2 nanotips as illustrated in Fig. 6 can be formed by firstly depositing a polystyrene (PS) sphere monolayer as a stencil mask and then depositing TiO_2 thorough the spacing between PS spheres [3]. The cross-sectional

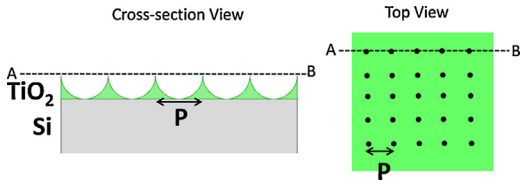

Fig. 6. Illustration of pseudo-graded index ARC using dielectric nanotips.

view is nano-island and the top view is nano-islands arranged in an array. When calculating the reflectance, the structure is ARC + Si + PML. When calculating the absorbance, the structure is ARC + 0.3 μmSi + Ag reflector. It is worth mention that dielectric nanotip shows a little higher reflectance compared to the planar multilayer ARC or the Si nanotips. This is due to the existence of heterogeneous interface between TiO_2 and silicon where perfect index grading is broken. Nonetheless, due to this TiO_2/Silicon interface, the severe photon outcoupling also disappears, evident from the reflectance plot in Fig. 7. In the absorbance plot in Fig. 7, the quasi-guided mode excitation is very pronounced, manifesting the superior light trapping property. Therefore, the pseudo-grade index ARC is more suitable for thin-film photovoltaics due to its superior mode excitation, but not suitable for wafer-based photovoltaics due to its higher reflectance resulted from a broken index grading. The normalized absorbance is 0.382. The integrated metal loss is 0.159.

4. Mode coupling approach

In contrast to the graded index approach where the physically graded layers are used to reduce the reflection of semiconductor–air interface, the gratings or other periodic structures can also be used. The physics of low reflectance for the mode coupling ARCs is the forward

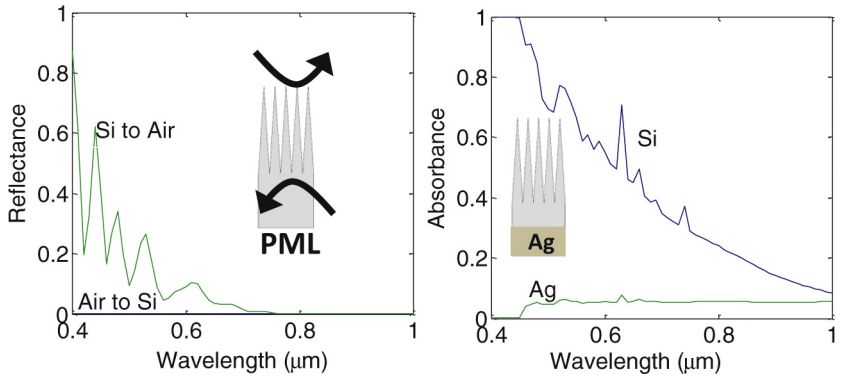

Fig. 5. Silicon nanotip purely GI ARC characteristic. (Left) reflectance from air to Si and reflectance from Si to air. (Right) absorbance for a stack of ARC, 0.3 μm Si and a silver reflector.

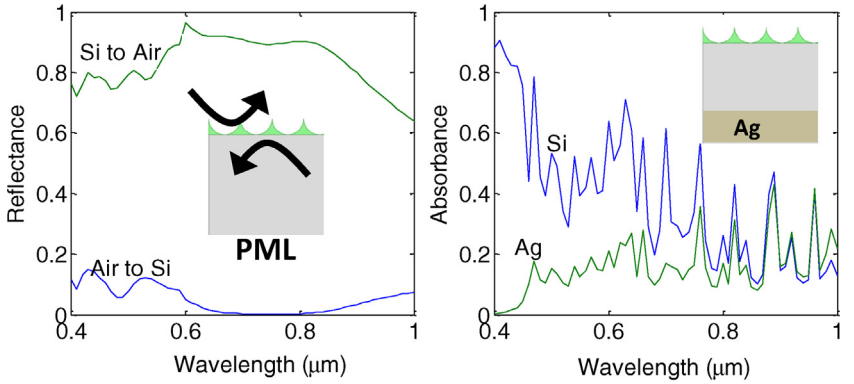

Fig. 7. Dielectric nanotip pseudo-GI ARC characteristic. (Left) reflectance from air to Si and reflectance from Si to air. (Right) absorbance for a stack of ARC, 0.3 μm Si and a silver reflector.

Table 1
Comparison of different anti-reflection coating.

Type of ARC	(Purely graded index) Multi-layer dielectric	(Purely graded index) Si nanotip	(Pseudo-graded index) TiO_2 nanotip	(Mode coupling) Mie scattering
Averaged reflectance, R_{avg}	4.39%	0.04%	4.87%	1.87%
Normalized silicon integrated absorbance (AM1.5)	0.119	0.159	0.381	0.380

diffraction orders initiated by the front surface grating, dielectric or metallic scatterers, or other nano-structures. In order to lower the reflectance, the forward diffraction power should be maximized. In the case where back reflector exists, i.e., absorbance calculation, the forward diffracted photons are coupled into the waveguide modes of the solar cell structures. ARCs that fall into this category include ZnO nanorods [5], surface plasmon metal spheres [6–9], grating couplers [10], and a recently proposed Mie scattering based structure [11]. The Mie scatterer as illustrated in Fig. 8 is selected as an example for mode coupling ARC. The cylindrically shaped Mie scatterers are formed by firstly dry

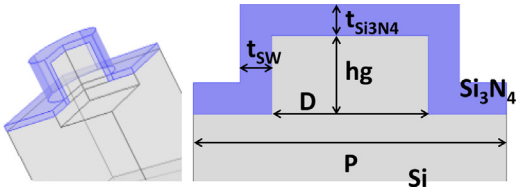

Fig. 8. Illustration of mode coupling ARC using Mie scattering.

etching the silicon. Afterward, conformal Si_3N_4 layer is deposited on top of silicon. The physics is that the nano-scaled dielectric scatterers initiate Mie modes and facilitate photon forward scattering and in-coupling into the semiconductor film [11,18]. The geometry is from

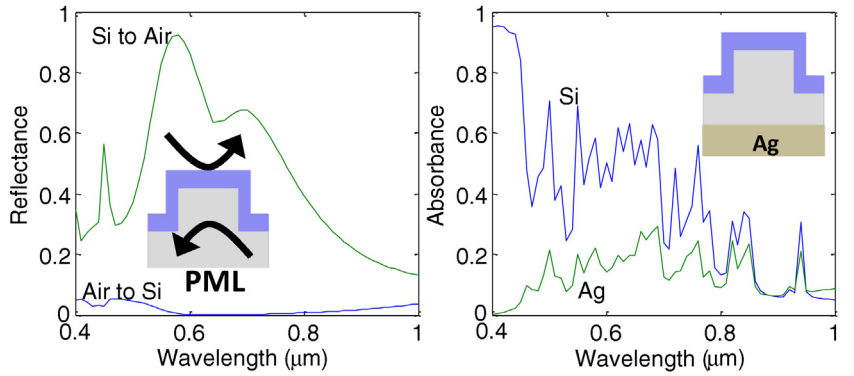

Fig. 9. Mie scattering mode coupling ARC characteristic. (Left) reflectance from air to Si and reflectance from Si to air. (Right) absorbance for a stack of ARC, 0.3 μm Si and a silver reflector. $P = 450$ nm, $t_{Si3N4} = 50$ nm, $h_g = 150$ nm, $D = 125$ nm, $t_{SW} = 75$ nm.

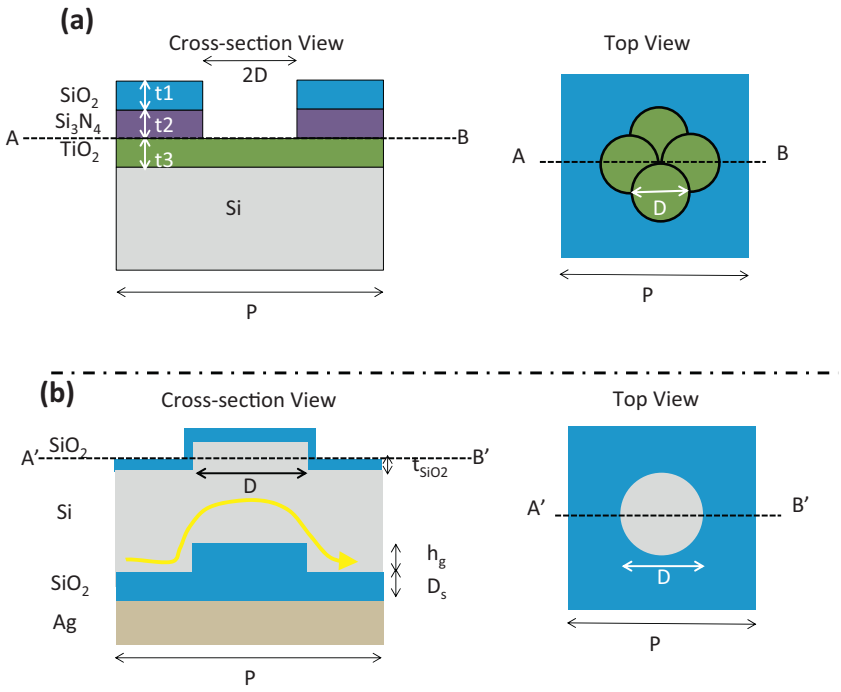

Fig. 10. (a) The pattern-designed air-hole anti-reflection coating. (b) The importance of bended light path for thin-film light trapping. The bottom grating is formed to bend the active silicon layer.

[11]. When calculating the reflectance, the structure is ARC + Si + PML. When calculating the absorbance the structure is ARC + 0.3 μmSi + Ag reflector. This class of ARC does not count on, or at least totally count on, index grading to achieve the low reflectance, and it is expected that the photon out-coupling will not be as pronounced as in purely graded index ARC. It can be seen from Fig. 9 that the reflectance is effectively reduced to <5% for the entire spectral range of interest. The reduction of reflection is because the silicon Mie scatterers effectively couple the photons into the forward propagation direction by mode coupling. In the case of a real solar cell where a back reflector exists, the dielectric scatterers will couple the photons into the Bloch propagation modes. On the contrary, the purely graded index ARC tends to couple the incident photons into leaky modes leading to the disappearance of guided mode excitations and degraded light trapping. This is evident from Fig. 9 where the reflectance from both air to Si and from Si to air is shown. In Fig. 9, the photon out-coupling disappears and the easy-in-easy-out nature associated with purely GI ARC no longer exists. From the spectral response it is seen that long wavelength quasi-guided mode excitation is very pronounced, manifesting the fact that the photons are effectively coupled into the Bloch propagation modes. The normalized integrated absorbance is 0.3797. The integrated metal loss is 0.14. Table 1 compares the normalized absorbance for different ARCs. It is worth mention purely graded index ARCs lead to low absorbance due to the annihilation of quasi-guided mode excitations.

5. A pattern-designed photonic crystal anti-reflection coating and the importance of bended light path

Fig. 10 illustrates a new type of anti-reflection coating with geometry optimization with a genetic algorithm. The design is air-hole photonic crystal with complex photonic pattern illustrated in Fig. 10(a). The cross-sectional view reveals that it is air-hole design with air void patterned in dielectric layers. The top view shows that the complex photonic pattern is formed and, therefore, the shape of air-holes consists of four green circles. This proposed structure demonstrates the importance of pattern design and geometry optimization. The optimized geometry in this case is $t_1 = 63$ nm, $t_2 = 84$ nm, $t_3 = 48$ nm, $P = 397$ nm, $D = 151$ nm, using genetic algorithm global optimization. The averaged reflectance is 0.81%, which is much lower than TiO_2 nano-tips and Mode coupling ARC evident from Table 1. The reflectance is slightly higher than ultra-long silicon nano-tip ARC in Section 3, but ultra-long silicon nano-tips is impractical due to severe surface recombination, bulky

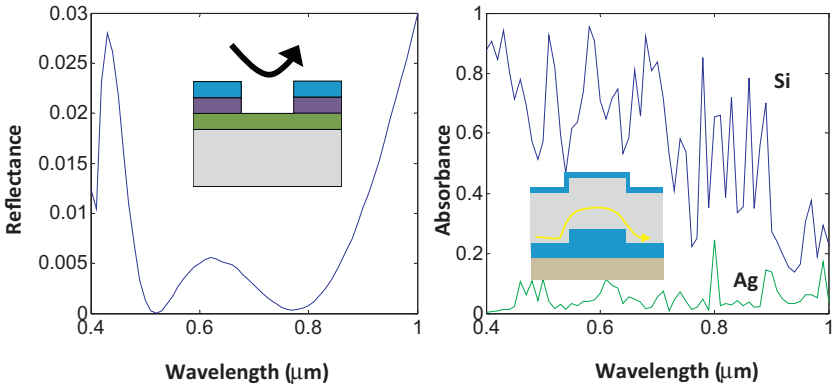

Fig. 11. The reflectance and absorbance plots for the structures proposed in Fig. 10(a) and (b), respectively. (Left) the reflectance from air to Si for Fig. 10(a). (Right) the absorbance for the structure in Fig. 10(b) with 0.3 μm Si and a silver reflector.

dimension, and poor light trapping, which are also evident from Table 1. In Fig. 10(b), we pinpoint that the key factor for thin-film solar cell light trapping is, in fact, the bended light path. In this scenario, the active silicon layer is no longer planar, and it is bended to enhance the effective path length for photons. In order to achieve bended silicon absorber, the bottom grating on SiO_2 layer is essential. As a result, in addition to the proper selection of ARC structure, the bended absorber is also critical for superior light trapping. The optimized geometry for this structure is $t_{SiO2} = 74$ nm, $h_g = 129$ nm, $D_s = 100$ nm, $P = 554$ nm, $D = 373$ nm. The integrated absorbance is 0.60, significantly higher than any value achieved in Table 1. In order to achieve a bended active absorber layer, deposition of silicon thin-film on a corrugated metal or glass substrate is feasible in practice during semiconductor processing. This leads to so-called substrate-type thin-film solar cells or superstrate-type thin-film solar cells. It should be pointed out that pattern design similar to Fig. 10(a) is also possible for Fig. 10(b), though a simple circularly shaped grating is used to isolate the effect of bended-light-path for photovoltaic light trapping (Fig. 11).

6. Conclusion

This work shows that the purely graded index (GI) anti-reflection coating (ARC) can degrade the long wavelength light trapping by annihilating guide mode excitation. The degraded light trapping is due to the easy-in easy-out nature of the physically index-graded ARC layers. This is confirmed by calculating the reflectance from air to silicon and from silicon to air through the graded index layer. It is found that purely graded index ARC results in photon out-coupling leading to photon escape from the active absorbing materials. ARC based on mode coupling does not suffer from easy-in easy-out problem and thus it can provide one-way photon pass which not only reduces air to silicon reflectance but prohibits silicon to air photon escape. The sidewall thickness of mode coupling ARCs is critical for its low reflectance characteristic and thus process methods should be carefully selected. This work identifies the one-way photon pass is the key factor to provide both low air-to-Si reflectance and strong long wavelength guided mode excitations for solar cells. It is suggested that the purely graded index ARC is more suitable for the case where the semiconductor thickness is thick enough to absorb sunlight in two photon traces, e.g., wafer-based solar cells. For pseudo-graded index ARC the perfect index grading is broken, and it is suitable for thin-film photovoltaics due to its superior mode excitation but not suitable for wafer-based photovoltaics due to its higher reflectance resulted from the broken index grading. Mode coupling ARC can be used for both wafer-based and thin-film applications since it provides low reflectance and preserves quasi-guided mode excitations. In the end, the photonic pattern-designed air-hole anti-reflection coating is proposed where the averaged reflectance is lower than previously proposed TiO_2 nano-tip ARC and Mie mode coupling ARC. In addition, the importance of bended light path for photovoltaic light trapping is pinpointed and the integrated absorbance achieved is >0.6 for only 0.3 μm active silicon layer.

References

[1] S. Chhajed, et al., Nanostructured multilayer graded-index antireflection coating for Si solar cells with broadband and omnidirectional characteristics, Appl. Phys. Lett. 93 (2008) 251108.
[2] Y.-F. Huang, et al., Improved broadband and quasiomnidirectional anti-reflection properties with biomimetic silicon nanostructures, Nat. Nanotechnol. 2 (2007) 770–774.

[3] P.C. Tseng, et al., Antireflection and light trapping of subwavelength surface structures formed by colloidal lithography on thin film solar cells, Prog. Photovolt. Res. Appl. 20 (2012) 135–142.
[4] N. Yamada, et al., Characterization of antireflection moth-eye film on crystalline silicon photovoltaic module, Opt. Express 19 (2012) A118–A125.
[5] L. Ae, et al., ZnO nanorod arrays as an antireflective coating for Cu(In,Ga)Se2 thin film solar cells, Prog. Photovolt. Res. Appl. 18 (2010) 209–213.
[6] S. Pillai, M.A. Green, Plasmonics for photovoltaic applications, Sol. Energy Mater. Sol. 94 (2010) 1481–1486.
[7] H.A. Atwater, A. Polman, Plasmonics for improved photovoltaic devices, Nat. Mater. 9 (2010) 205–213.
[8] K.R. Catchpole, A. Polman, Plasmonic solar cells, Opt. Express 16 (2008) 21793–21800.
[9] S. Pillai, et al., The effect of dielectric spacer thickness on surface plasmon enhanced solar cells for front and rear side depositions, J. Appl. Phys. 109 (2011) 073105.
[10] H. Stiebig, et al., Silicon thin-film solar cells with rectangular-shaped grating couplers, Prog. Photovolt. Res. Appl. 14 (2006) 13–24.
[11] P. Spinelli, et al., Broadband omnidirectional antireflection coating based on subwavelength surface Mie resonators, Nat. Commun. 3 (2012) 692.
[12] U.W. Paetzold, et al., Design of nanostructured plasmonic back contacts for thin-film silicon solar cells, Opt. Express 19 (2011) A1219–A1230.
[13] P. Bhattacharya, Semiconductor Optoelectronic Devices, 2nd ed., Prentice-Hall, Upper Saddle River, NJ, 2006.
[14] C. AB, Comsol Multiphysics RF Module User Guide V 3.3, 2006.
[15] Synopsys, Sentaurus Device EMW User Manual V. X-2005, 10th ed., 2005, pp. 78–79.
[16] Rsoft, Rsoft CAD User Manual 8.2, Rsoft Design Group, New York, 2010.
[17] A. Lin, J.D. Phillips, Optimization of random diffraction gratings in thin-film solar cells using genetic algorithms, Sol. Energy Mater. Sol. 92 (2008) 1689–1696.
[18] S.A. Mann, et al., Dielectric particle and void resonators for thin film solar cell textures, Opt. Express 19 (2011) 25729–25740.